Histone Deacetylase Is a Target of Valproic Acid-Mediated Cellular Differentiation

Nadia Gurvich,[1] Oxana M. Tsygankova,[1] Judy L. Meinkoth,[1] and Peter S. Klein[2]

[1]Department of Pharmacology and [2]Howard Hughes Medical Institute and Department of Medicine, Division of Hematology-Oncology, University of Pennsylvania School of Medicine, Philadelphia, Pennsylvania

ABSTRACT

Valproic acid (VPA), a well-established therapy for seizures and bipolar disorder, has recently been shown to inhibit histone deacetylases (HDACs). Similar to more widely studied HDAC inhibitors, VPA can cause growth arrest and induce differentiation of transformed cells in culture. Whether this effect of VPA is through inhibition of HDACs or modulation of another target of VPA has not been tested. We have used a series of VPA analogs to establish a pharmacological profile for HDAC inhibition. We find that VPA and its analogs inhibit multiple HDACs from class I and class II (but not HDAC6 or HDAC10) with a characteristic order of potency *in vitro*. These analogs also induce hyperacetylation of core histones H3 and H4 in intact cells with an order of potency that parallels *in vitro* inhibition. VPA and VPA analogs induce differentiation in hematopoietic cell lines in a p21-dependent manner, and the order of potency for induction of differentiation parallels the potencies for inhibition *in vitro*, as well as for acetylation of histones associated with the p21 promoter, supporting the argument that differentiation caused by VPA is mediated through inhibition of HDACs. These findings provide additional evidence that VPA, a well-tolerated, orally administered drug with extensive clinical experience, may serve as an effective chemotherapeutic agent through targeting of HDACs.

INTRODUCTION

Valproic acid (VPA; 2-propyl-pentanoic acid) is a short-chain branched fatty acid that was discovered serendipitously as an anticonvulsant in 1962 while being used as a solvent for experimental anticonvulsants (1). VPA is used today to treat a variety of seizure disorders as well as bipolar disorder (manic depressive illness). The mechanisms of action for VPA in bipolar disorder and epilepsy are currently unknown, although a number of targets have been proposed (1, 2).

Recently, VPA was shown to inhibit histone deacetylases (HDACs) at therapeutic concentrations (3, 4). Acetylation of the NH_2-terminal tails of core histones is central to the specification of a "histone code" that influences the expression of target genes (5). Recruitment of histone acetyltransferases by transcription factor complexes is associated with a more open DNA conformation that, in general, facilitates transcription of target genes. Conversely, deacetylation of core histones by HDACs is associated with a "closed" chromatin conformation and (in general) repression of transcription. Therefore, inhibition of HDACs typically leads to derepression of transcription.

HDACs are subdivided into three classes. Class I HDACs (including HDACs 1–3 and 8) are similar to yeast RPD3 and are found in complexes containing corepressors N-CoR, Sin3, and SMRT as well as methyl-binding proteins such as MeCP2. Class II HDACs (including HDACs 4–7 and 9–11) are similar to yeast HDA1, have unique NH_2-terminal sequences, can shuttle between the nucleus and the cytoplasm, and may have roles distinct from class I HDACs. Class III-Sir2 family HDACs, which were described more recently, have significantly divergent amino acid sequences and, unlike class I and II HDACs, are nicotineamide dinucleotide dependent (6).

HDAC inhibitors from diverse origins arrest cell growth and induce differentiation in various *in vitro* and *in vivo* models including acute promyelocytic leukemia and in cell lines derived from colon, lung, and prostate carcinomas (7). HDAC inhibitors have thus been proposed as promising anticancer therapies, and several are currently in Phase I and Phase II clinical trials (7–10). Indeed, VPA can induce differentiation of cell lines derived from neuroblastoma, glioma, and teratocarcinoma (11, 12) and leukemic blasts isolated from patients with newly diagnosed acute myeloid leukemia (4). However, it is not known whether the putative antineoplastic effects of VPA are mediated through inhibition of HDACs or through another target of VPA. To address this question, we have used a series of VPA analogs to establish a pharmacological profile for HDAC inhibition *in vitro* and in cultured cells. We find that VPA and VPA analogs inhibit multiple class I and class II HDACs with a similar order of potency. Furthermore, VPA and its analogs induce differentiation of hematopoietic cell lines with an order of potency that parallels inhibition of HDACs *in vitro* and *in vivo*. These findings support the hypothesis that VPA induces differentiation of transformed cells through inhibition of HDACs and support the use of VPA as an alternative HDAC inhibitor in the therapy of human malignancies.

MATERIALS AND METHODS

Reagents and Plasmids. Valpromide (VPM) was a gift from Katwijk Chemie B.V. (Katwijk, the Netherlands). 2-Methyl-2-propylpentanoic acid (2M2PP) was synthesized by Richman Chemical Inc. (Lower Gwynedd, PA). 2-Methyl-2-pentenoic acid (2M2P) and 4-pentenoic acid (4PA) were purchased from Alpha Aesar (Ward Hill, MA). 2-Ethylhexanoic acid (2EH), VPA (sodium salt), and butyric acid (sodium salt) were purchased from Sigma-Aldrich (St. Louis, MO). The structures of VPA analogs used in this work are shown in Fig. 1. The following plasmids were kindly provided by several investigators: HDAC1 and HDAC3 (Tony Kouzarides; The Wellcome/Cancer Research United Kingdom Institute, Cambridge, United Kingdom); HDAC2 (Ed Seto; University of Florida); HDACs 4, 5, and 6 (Stuart Schreiber; Harvard University); HDAC7 (Eric Verdin; University of California, San Francisco, CA); and HDAC10 (Tso-Pang Yao; Duke University).

Cell Culture. K562, U937, and 293T cell lines were obtained from American Type Culture Collection (Manassas, VA). Stable U937 cell lines expressing p21 antisense RNA or empty vector were kindly provided by Steven Grant (University of Virginia). K562 and U937 cells were grown in RPMI 1640 with 10% fetal bovine serum. For flow cytometry (FCM) assays, U937 cells were seeded at 10^5 cells/ml in 2 ml of culture medium and treated with VPA and analogs (0.25–2 mM) for 6 days. For all differentiation assays, K562 cells were seeded at 5×10^4 cells/ml in 2 ml of culture medium and treated with VPA and analogs (0.25–2 mM) for 3 days. Wistar rat thyroid (WRT) cells were grown in 3H (Coon's modified Ham's F-12 medium, 5% calf serum, 2 mM glutamine, 0.15% $NaHCO_3$, 1 milliunit/ml TSH, 10 μg/ml insulin, and 5 μg/ml transferrin) and starved in basal medium (Coon's modified Ham's F-12 medium, 2 mM glutamine, 0.15% $NaHCO_3$, and 1 mM HEPES) for 3 days before treatment. 293T cells were grown in DMEM with 10% fetal bovine serum and seeded at 3×10^6 cells/100-mm plate for transfection.

HDAC Assay. HDAC activity was measured *in vitro* using a commercial assay kit (Biomol, Plymouth Meeting, PA) in which fluorescent product is generated from a synthetic, acetylated substrate on deacetylation. 293T cells were transfected with 5 μg of plasmids encoding myc- or FLAG-tagged HDAC preincubated with 15 μl of FuGENE 6 transfection reagent (Roche,
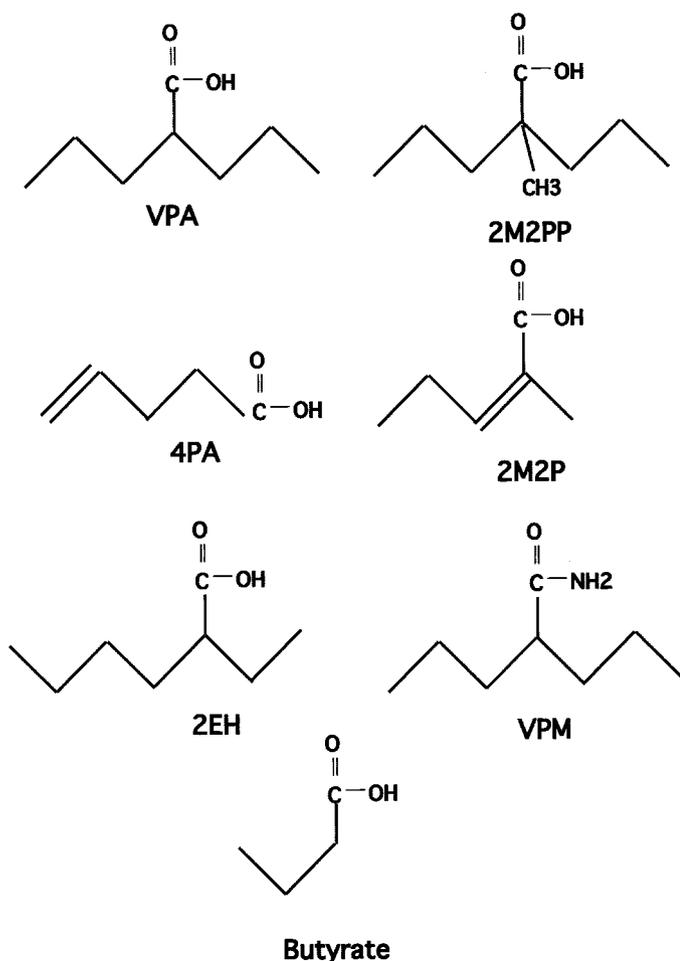
Fig. 1. Structures of valproic acid and analogs. *VPA*, valproic acid; *2M2PP*, 2-methyl-2*n*-propylpentanoic acid; *4PA*, 4-pentenoic acid; *2M2P*, 2-methyl-pentenoic acid; *2EH*, 2-ethylhexanoic acid; *VPM*, valpromide.

Indianapolis, IN). After 24 h, cells were harvested in reporter lysis buffer (Promega, Madison, WI) supplemented with protease inhibitor mixture (Sigma-Aldrich), and HDACs were immunoprecipitated overnight with myc- or FLAG-agarose beads [Santa Cruz Biotechnology (Santa Cruz, CA) and Sigma-Aldrich, respectively]. The following day, the beads were washed three times and resuspended in a volume of HDAC buffer [25 mM Tris/Cl (pH 8.0), 137 mM NaCl, 2.7 mM KCl, and 1 mM MgCl$_2$] to achieve at least 10-fold higher fluorescence over the basal fluorescence (beads incubated with untransfected cells) in samples without inhibitor. The assay was conducted at room temperature according to the manufacturer's protocol. The samples were prepared in triplicate and incubated for 15 min, and the fluorescence was measured on a fluorescence counter (Packard) within 30 min after stopping the reaction.

Immunoblotting. K562, U937, or WRT cells were seeded at 5×10^5 cells/ml in 10 ml, treated with VPA or analogs (0.25–2 mM) for the times indicated below, and harvested in reporter lysis buffer with protease inhibitor mixture. Protein concentration was measured with Bradford reagent (Bio-Rad, Hercules, CA); samples were adjusted to equal protein concentrations and then mixed with Laemmli sample buffer and separated on 10% or 15% SDS-PAGE gels. The gels were immunoblotted with antibodies for p21 (1:1000; Upstate Biotechnology, Lake Placid, NY), gelsolin (1:1000; Sigma), hnRNP-K (1:2000; a gift from Gideon Dreyfuss; University of Pennsylvania), actin (1:1000; Santa Cruz Biotechnology), or phosphorylated mitogen-activated protein kinase [MAPK (1:3000; Cell Signaling, Beverly, MA), and immunoblots were developed with the ECL Plus kit (Amersham, Piscataway, NJ) and visualized by exposure to x-ray film.

Isolation of Histones and Assay for Histone Acetylation. K562 or U937 cells were seeded at 5×10^5 cells/ml in 10 ml, treated with VPA or VPA analogs for the indicated times, and harvested in 200 μl of reporter lysis buffer.

Nuclei were collected by centrifugation at 14,000 rpm for 5 min at 4°C, and histones were extracted by shaking in 0.5 ml of 0.4 N sulfuric acid for 1 h at 4°C. The samples were centrifuged, and histones were precipitated from supernatants with 1 ml of ethanol for 1 h at –20°C, washed once with ethanol, and resuspended in 200 μl of Laemmli buffer. Twenty μl of each sample were electrophoresed on a 15% SDS-PAGE gel. Histone acetylation was determined by immunoblotting with antibodies to acetylated histones H3 and H4 (Upstate Biotechnology). Histone recovery was assessed by immunoblotting with an antibody to histone H4 (Upstate Biotechnology) and by staining the gels with Coomassie Brilliant Blue.

Luciferase Assay. 293T cells were transfected with 5 μg of the SV40 luciferase reporter plasmid and, after 24 h, split into 6-well plates. The next day, cells were treated with VPA and analogs for 24 h. The cells were harvested in 0.5 ml of reporter lysis buffer with protease inhibitor mixture, and luciferase activity was measured using a luciferase assay kit (Promega).

Chromatin Immunoprecipitation (ChIP) Assay. The ChIP assay was performed as described previously (13, 14), with minor modifications. K562 cells were treated with VPA and analogs (2 mM each) for 24 h, cross-linked with 1% formaldehyde for 15 min at room temperature, washed twice in ice-cold PBS, incubated on ice in lysis buffer [1% SDS, 10 mM EDTA, and 50 mM Tris-HCl (pH 8.1)] with protease inhibitor mixture, and sonicated 10 times for 10 s, followed by centrifugation at $14,000 \times g$ for 15 min. The supernatants were collected and diluted 10-fold in dilution buffer [0.01% SDS, 1.1% Triton X-100, 1.2 mM EDTA, 16.7 mM Tris-HCl (pH 8.1), and 167 mM NaCl] with protease inhibitor mixture. Two percent of the supernatant fraction was saved to quantitate the amount of input DNA, and the rest was precleared with 60 μl of salmon sperm DNA and protein A-agarose (Invitrogen) as a 50% slurry in 10 mM Tris-HCl (pH 8.1)-1 mM EDTA for 30 min at 4°C and immunoprecipitated with antibody to acetylated histone H4 (Upstate Biotechnology) or control rabbit IgG (Caltag) overnight. The immunoprecipitates were collected with 60 μl of salmon sperm DNA/protein A slurry and washed sequentially for 30 min at 4°C in low-salt wash buffer [0.1% SDS, 1% Triton X-100, 2 mM EDTA, 20 mM Tris-HCl (pH 8.1), and 150 mM NaCl], high-salt wash buffer [0.1% SDS, 1% Triton X-100, 2 mM EDTA, 20 mM Tris-HCl (pH 8.1), and 500 mM NaCl], LiCl wash buffer [0.25 M LiCl, 1% NP40, 1% deoxycholate, 1 mM EDTA, 10 mM Tris-HCl (pH 8.1)], and Tris-EDTA buffer. The DNA was eluted in 100 μl of elution buffer (1% SDS and 0.1 M NaHCO$_3$) for 30 min at room temperature, incubated overnight in 5 M NaCl at 65°C to reverse the cross-links, and purified using PCR purification kit (Qiagen).

Real-Time PCR Analysis. The DNA from the input and immunoprecipitated fractions was analyzed by real-time PCR on the LightCycler PCR system (Roche) using SYBR Green dye (Molecular Probes, Eugene, OR) and the following primers for the p21 promoter: 5′-TCT-TTT-CAG-CTG-CAT-TGG-GTA-A-3′ and 5′-GCC-CCC-TTT-CTG-GCT-CA-3′ (13). The concentrations of the ChIP and input samples were calculated from a standard curve generated with p21 primers and the input DNA, and the ChIP samples were normalized by the corresponding input samples.

Reverse Transcription-PCR Analysis of p21 Expression. K562 cells were treated with VPA and analogs, as described for ChIP assay above, and RNA was harvested at 24 h. cDNA was synthesized using Moloney murine leukemia virus reverse transcriptase (Invitrogen) and used in real-time PCR with SYBR Green dye and p21 primers (5′-CTG-GAG-ACT-CTC-AGG-GTC-GAA-3′ and 5′-CGG-CGT-TTG-GAG-TGG-TAG-AA-3′) as described previously (13) or β-actin primers (5′-GCT-CGT-CGT-CGA-CAA-CGG-CTC-3′ and 5′-CAA-ACA-TGA-TCT-GGG-TCA-TCT-TCT-C-3′). The concentrations of PCR products were calculated from the standard curves established for each primer pair, and the amount of p21 product was normalized to the amount of β-actin product.

Differentiation Markers. Markers of differentiation were assessed by FACS using antibodies to CD11a, CD11b, CD11c, CD13, CD18, CD41, CD45, CD64, HLA-DR, and glycophorin A [all antibodies for FCM were from Caltag (Burlingame, CA)]. Cells (2.5×10^5) in 50 μl of MACS buffer (PBS/0.5% BSA/5 mM EDTA) were incubated with 100 μg/ml mouse IgG reagent (Sigma) at 4°C for 15 min to reduce nonspecific antibody staining; stained for 30 min at 4°C with 5 μl of FITC-, phycoerythrin-, or tricolor-conjugated antibodies against differentiation markers or isotype-matched controls; washed twice with MACS buffer; and incubated with 2 μg/ml propidium iodide for 5 min to exclude dead cells from analysis. For detection of fetal hemoglobin, 2.5×10^5 cells were stained with 5 μl of FITC-coupled anti-fetal

hemoglobin antibody according to the manufacturer's protocol (Caltag). Cells were analyzed by FCM, and the percentage of positive cells or mean intensity was plotted to quantify expression of differentiation markers. For benzidine staining, K562 cells were washed once with PBS and resuspended in 0.5 ml of PBS. A total of 0.5 ml of 0.2% tetramethylbenzidine reagent (Sigma) in 0.5 M acetic acid, with 2% H_2O_2 added just before use, was added to cells and incubated for 30 min in the dark at room temperature.

RESULTS

Inhibition of Class I and Class II HDACs *in Vitro* by VPA. VPA (Fig. 1) has previously been shown to inhibit a subset of HDACs *in vitro* (3, 4). To extend this analysis, additional HDACs from classes I and II were tested with VPA in an *in vitro* deacetylation assay using a synthetic, acetylated substrate that becomes fluorescent on deacetylation by HDACs (15). Myc or FLAG-tagged HDACs were expressed in 293T cells and immunoprecipitated with epitope-specific antibodies. The presence of HDACs in the immune complexes was verified by Western blot with myc or FLAG antibodies (data not shown). The beads containing HDAC immune complexes were then assayed in the presence of VPA (0.1–20 mM). HDAC activities of the samples with inhibitor are represented as the percentage of HDAC activity in the absence of inhibitor and plotted *versus* the concentrations of VPA to determine the concentration that inhibits 50% (IC_{50}) of the activity for each HDAC. VPA inhibits class I HDACs (HDACs 1–3) with IC_{50} values ranging from 0.7 to 1 mM and inhibits class II subclass I HDACs 4, 5, and 7 with IC_{50} values ranging from 1 to 1.5 mM; surprisingly, VPA did not inhibit HDACs 6 or 10 (class II subclass II) under these assay conditions (Fig. 2A; Table 1). As a positive control,

Table 1 *Inhibition of class I and II HDACs[a] by VPA*

HDACs were expressed in 293T cells, immunoprecipitated, and tested with VPA in the *in vitro* HDAC assay (as described in Fig. 2); the means for HDAC activity at each concentration of inhibitor from three independent experiments were plotted and used to calculate IC_{50} values for each HDAC.

Class	Enzyme	IC_{50} (mM)
I	HDAC1	0.7
I	HDAC2	0.8
I	HDAC3	1
II subclass I	HDAC4	1.5
II subclass I	HDAC5	1
II subclass II	HDAC6	>20
II subclass I	HDAC7	1.3
II subclass II	HDAC10	>20

[a] HDAC, histone deacetylase; VPA, valproic acid.

HDAC6 and HDAC10 were inhibited by the conventional HDAC inhibitor trichostatin A (TSA; data not shown). Thus, VPA appears to be a more selective HDAC inhibitor than TSA, similar to findings with sodium butyrate (16, 17), and could be used to distinguish the roles of HDAC6 and HDAC10 from other HDACs.

Inhibition of HDACs by VPA Analogs. A series of VPA analogs has been used to define the structural features of VPA that are responsible for its anticonvulsant activity, teratogenic potential, and activation of peroxisome proliferator-activated receptor δ (PPARδ)-dependent transcription (18, 19). The relative teratogenic potential of VPA analogs correlated with activation of the PPARδ reporter, but anticonvulsant activity was clearly distinct based on the response profile for this analog series. More limited analyses also indicate that the potency in HDAC inhibition correlates with teratogenic potential (3, 4). We have therefore used this pharmacological approach to further characterize the structural characteristics of VPA that correlate with inhibition of HDACs. The structures of VPA and the analogs used in this work are shown in Fig. 1. Butyrate, a commonly used HDAC inhibitor, is also structurally similar to VPA, except that the carbon chain is shorter and unbranched.

These VPA analogs were tested in the *in vitro* HDAC assay using HDAC1, as described above. Butyrate and VPA were the most potent inhibitors of HDAC1 (Fig. 2B). The IC_{50} values for 4PA and 2EH were approximately 2.3 mM, 2M2PP inhibited less potently than 4PA and 2EH (IC_{50} = ~7.5 mM), and inhibition by VPM and 2M2P was minimal (IC_{50} = 15 mM for 2M2P, IC_{50} > 20 mM for VPM; Table 2). Similar relative potencies of these analogs were observed for inhibition of HDAC2 and HDAC7, except that these two HDACs appeared to be more sensitive to 4PA (Table 2). When endogenous HDAC activity in HeLa cell nuclear extracts was assayed in the presence of VPA analogs, the relative inhibitory potency of the analogs was similar to inhibition of HDAC1, although the IC_{50} values for the HeLa nuclear extract were higher than those for HDAC1, suggesting that other HDACs present in HeLa cells are less effectively inhibited by VPA and VPA analogs (Refs. 3 and 4; data not shown). Similar to VPA, 2EH and 4PA did not inhibit HDACs 6 and 10 (data not shown); these HDACs may contribute to the HDAC activity present in HeLa cell nuclear extracts. To summarize, the order of potency of VPA analogs for inhibition of HDACs 1, 2, and 7 (as well as HDAC activity in HeLa nuclear extracts) is as follows: butyrate > VPA > 2EH > 4PA > 2M2PP > 2M2P > VPM (Fig. 2B; Table 2).

Inhibition of HDACs by VPA Analogs in Cultured Cells. To verify that the *in vitro* effects of VPA analogs reflect their ability to inhibit HDACs in intact cells, the compounds were further tested by measuring acetylation of endogenous histones in the hematopoietic K562 and U937 cell lines. Acetylation of core histones H3 and H4 was assayed by Western blot of acid-extracted nuclei using antibodies that specifically recognize acetylated histone NH_2-terminal tails (20).
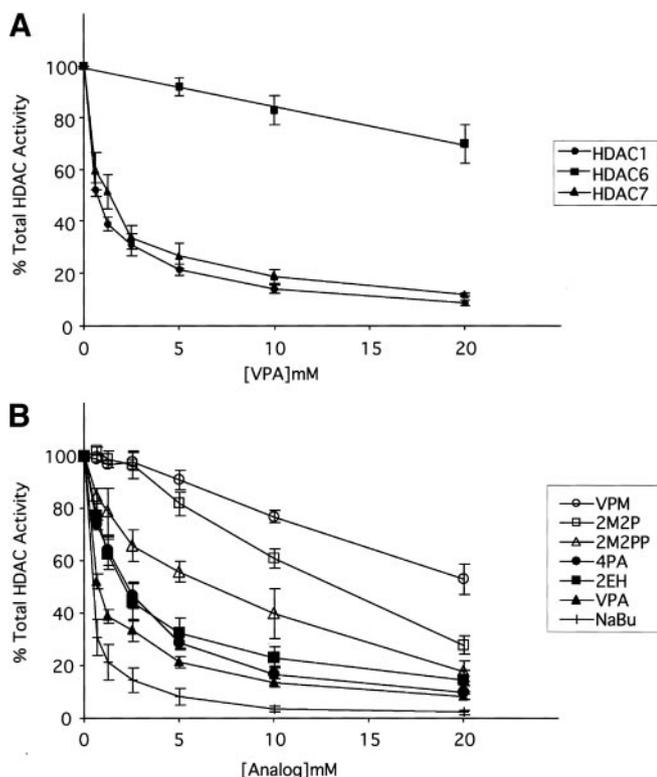
Fig. 2. Inhibition of histone deacetylases (HDACs) from class I and II *in vitro* by valproic acid (VPA) and analogs. *A,* epitope-tagged HDACs 1, 6, and 7 were expressed in 293T cells, immunoprecipitated, and assayed for HDAC activity *in vitro* in the presence of 0.3–20 mM VPA. HDAC activity is represented as a percentage of total activity of each HDAC. Each *data point* shown represents the mean HDAC activity from at least three independent experiments. *B,* Myc-tagged HDAC1 was expressed in 293T cells, immunoprecipitated, and assayed with each of the VPA analogs (0.1–20 mM); the means of at least three experiments were plotted.

Table 2 *Inhibition of class I and II HDACs[a] by VPA analogs*

Immunoprecipitated HDACs were tested with VPA analogs in the *in vitro* HDAC assay (as above); the means for HDAC activity at each concentration of inhibitor from three independent experiments were plotted and used to calculate IC_{50} values for each HDAC (as described in Fig. 2 and Table 1). Endogenous HDAC activity in HeLa cell nuclear extracts was also assayed with each inhibitor.

Inhibitor	HDAC (IC_{50}, mM)		
	HDAC1	HDAC2	HDAC7
NaBu	0.3	0.4	0.3
VPA	0.7	0.8	1.3
4PA	2.3	1	1
2EH	2.3	2.5	1.9
2M2PP	7.5	7.8	8.5
2M2P	15	15	15
VPM	>20	>20	>20

[a] HDAC, histone deacetylase; NaBu, sodium butyrate; VPA, valproic acid; 4PA, 4-pentenoic acid; 2EH, 2-ethylhexanoic acid; 2M2PP, 2-methyl-2-propylpentanoic acid; 2M2P, 2-methyl-2-pentenoic acid; VPM, valpromide.
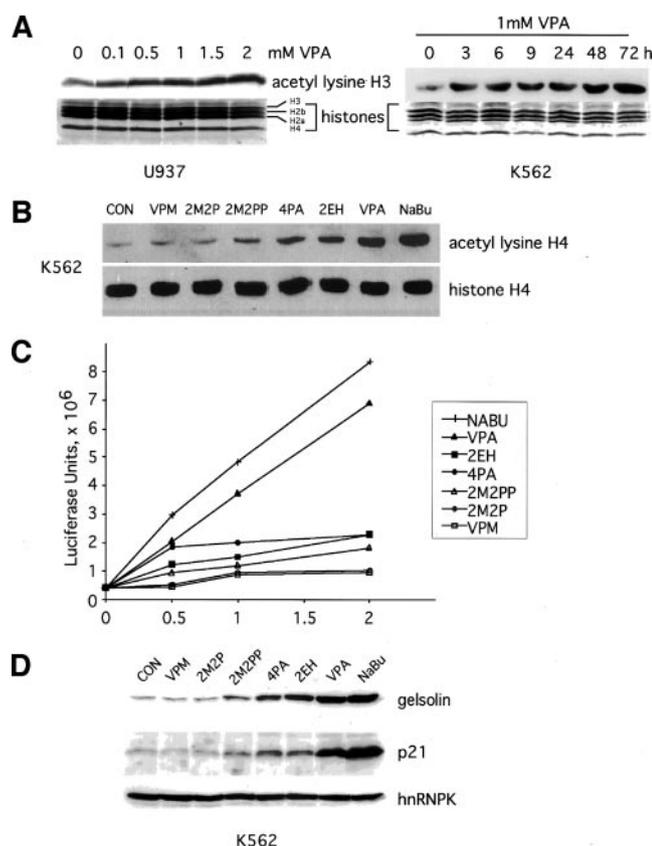

Fig. 3. Inhibition of histone deacetylases by valproic acid (VPA) and VPA analogs in cultured cells. *A*, U937 cells were treated with 0.1–2 mM VPA for 18 h to show the dose response for histone acetylation (*left panel*). K562 cells (*right panel*) were treated with 1 mM VPA and harvested at the indicated time points to evaluate the time course for histone hyperacetylation by VPA. In each case, histones were isolated and immunoblotted for acetylated histone H3 or stained with Coomassie Blue to show the total amount of histones in each sample. *B*, K562 cells were treated with 2 mM VPA analogs for 24 h; histones were isolated and immunoblotted for acetylated histone H4 and total histone H4. *C*, 293T cells were transfected with the SV40-luciferase reporter, and the next day, cells were split into 6-well plates and treated with 0.5–2 mM VPA analogs for 24 h. Luciferase activity was measured in cell lysates and plotted as relative luciferase units. *D*, K562 cells were treated with 1 mM VPA and analogs for 24 h. The cell lysates were immunoblotted for p21, gelsolin, and hnRNP-K (loading control).

VPA increased acetylation of histone H3 in U937 and K562 cells (Fig. 3*A*) as well as H4 (Fig. 3*B*; data not shown) without affecting the overall level of histones. Furthermore, increased histone acetylation was evident within 3 h and persisted for as long as 72 h in the presence of VPA (Fig. 3*A*), whereas the acetylation of H3 and H4 induced by TSA was more transient, reaching a maximum at 4–8 h and returning to baseline by 24 h (Ref. 21; data not shown). VPA analogs 4PA,

2EH, and, to a lesser extent, 2M2PP also caused increased histone acetylation in K562 cells (Fig. 3*B*) and U937 cells (data not shown), whereas VPM and 2M2P did not appear to increase histone acetylation. Similar results were observed for histone H3 in both cell types (data not shown). Thus, the potency of these analogs in intact cells parallels their potency to inhibit HDACs *in vitro*.

HDAC inhibitors from diverse sources can activate multiple exogenous reporter genes, presumably through de-repression; for example, VPA induces transcription of PPARδ, lymphoid enhancer factor/T-cell factor, cytomegalovirus, and SV40 reporters (3, 4). Thus, induction of transcription from the SV40 luciferase reporter by VPA and VPA analogs was measured in 293T cells. As shown in Fig. 3*C*, the potency of VPA analogs to activate this reporter correlated with their ability to inhibit HDACs *in vitro* and to induce hyperacetylation of histones in cultured cells (Fig. 3*B*). HDAC inhibitors such as TSA, trapoxin, and butyrate also increase transcription of endogenous genes such as p21 and gelsolin (7, 8, 13, 14, 22). We therefore tested the ability of VPA and analogs to induce p21 and gelsolin in K562 and U937 cells. VPA and VPA analogs induced gelsolin in K562 cells (Fig. 3*D*) and U937 cells (data not shown) with an order of potency that paralleled the potency of these analogs in HDAC inhibition. VPA and VPA analogs also induced p21 in K562 cells (Fig. 3*D*) and in U937 cells (Fig. 7*A*) with a similar order of potency. This increase in p21 protein expression also correlated with the ability of VPA and VPA analogs to activate transcription of p21, as determined by real-time reverse transcription-PCR, and to cause increased acetylation of histone H4 associated with the p21 promoter, as measured by ChIP assay (Fig. 4). Thus, multiple independent measures in intact cells paralleled the order of HDAC inhibition by VPA analogs *in vitro*. This effect of VPA on acetylation of the p21 promoter is similar to the effect of other HDAC inhibitors (7, 8, 13, 14, 22) and supports the argument that the VPA-mediated increase in p21 expression is due to inhibition of HDACs.

Induction of Differentiation in U937 cells by VPA and VPA Analogs. To compare the effects of VPA and VPA analogs on cellular differentiation, we first analyzed U937 cells, which are frequently used as a model of myelomonocytic leukemia. U937 cells can be induced to differentiate toward the monocytic lineage by treatment
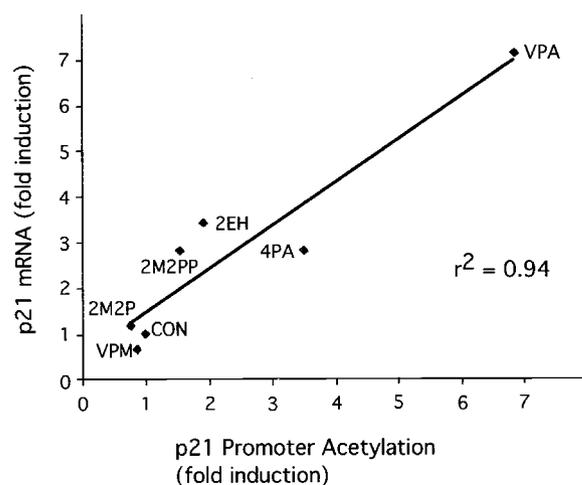

Fig. 4. Acetylation p21 promoter-associated histones and induction of p21 mRNA after treatment with valproic acid and analogs. K562 cells were treated with valproic acid and analogs for 24 h and evaluated for acetylation of histone H4 associated with the p21 promoter by chromatin immunoprecipitation assay (quantitated by real-time PCR) or for mRNA levels by real-time reverse transcription-PCR. The fold increase in acetylation of p21 promoter-associated histone H4 was plotted on the *X* axis, and the fold induction of p21 mRNA levels was plotted along the *Y* axis. Data are represented as the means of triplicate assays in each case. The experiments were repeated either three (chromatin immunoprecipitation) or two (reverse transcription-PCR) times with similar results.
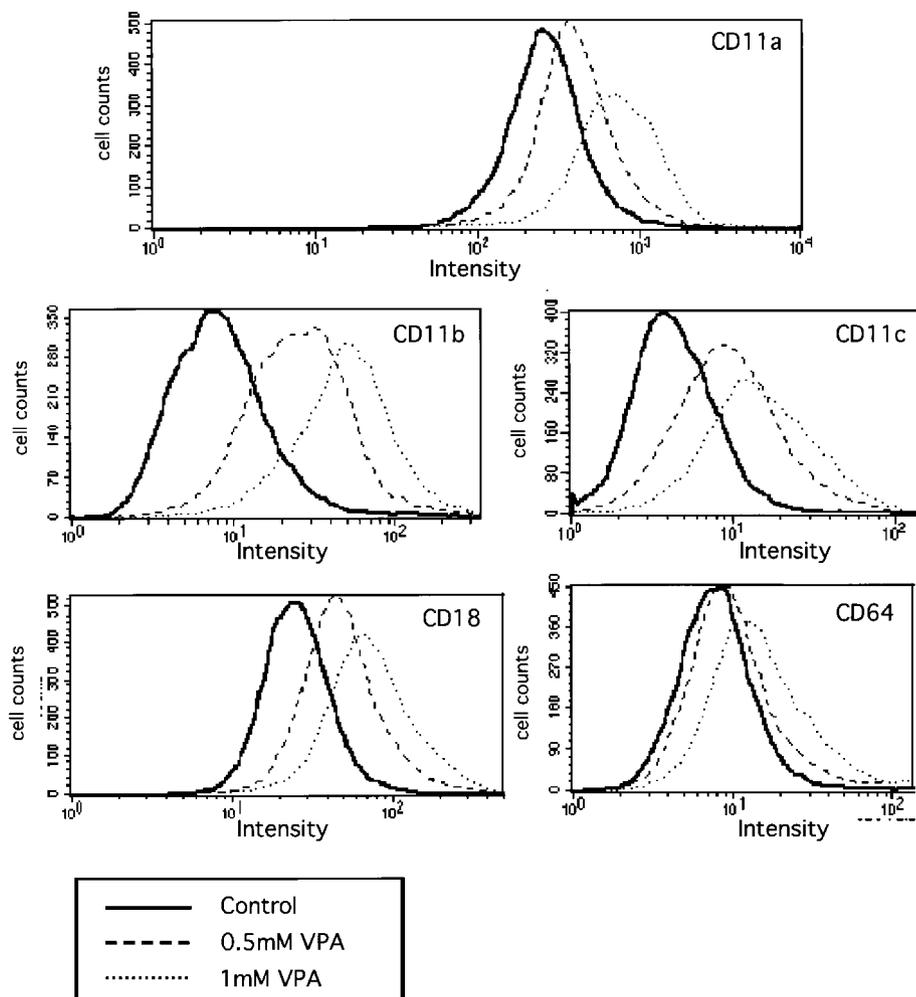
Fig. 5. Valproic acid (VPA) induces differentiation in U937 cells. U937 cells were treated with VPA for 6 days and analyzed for expression of CD11a, CD11b, CD11c, CD18– and CD64 surface markers by FCM. The histograms are shown for cells treated with 0 (*solid lines*), 0.5 (*dashed lines*), and 1 mM VPA (*dotted lines*) and are representative of at least three independent experiments for each marker.

with diverse compounds including ligands for nuclear hormone receptors (such as vitamin D_3 and retinoic acid), phorbol esters, and growth factors (such as transforming growth factor $\beta1$, granulocyte macrophage colony-stimulating factor, and IFN-γ). U937 cells were treated with VPA (0.25–1 mM), and the expression of differentiation markers was assessed by flow cytometry. Treatment with VPA for 6 days induced the myeloid differentiation markers CD11a, CD11b, CD11c, CD18 (Fig. 5), and CD13 (Fig. 6); the monocytic marker CD64 (Fig. 5); and HLA-DR (a marker of antigen-presenting cells including monocytes; Fig. 6). The potency of VPA analogs in the induction of CD11b, CD13, and HLA-DR expression was also tested and correlated with their ability to inhibit HDACs *in vitro* and in cultured cells (Fig. 7). Thus, VPA treatment induced an increase in the percentage of CD11b-positive cells by up to 32-fold; 2M2PP, 4PA, and 2EH had an intermediate effect; and 2M2P and VPM had no apparent effect. These observations support the proposal that VPA-induced differentiation of U937 cells is mediated through inhibition of HDACs.

The Role of p21 in the Induction of Differentiation in U937 Cells. Differentiation induced by HDAC inhibitors appears to be mediated in part through p21 (23, 24), an inhibitor of cell cycle-dependent protein kinases that is commonly induced by HDAC inhibitors, as described above (7, 8). Consistent with this, VPA caused a dose-dependent increase in p21 expression in U937 cells that was detectable within 24 h (Fig. 7A; see also Fig. 3D). To investigate the role of p21 in VPA-induced differentiation, induction of CD11b expression by VPA was assessed in U937 cell lines lacking p21

because previous work has shown that loss of p21 in these cells blocks butyrate-induced differentiation (24). p21 protein was induced by VPA in control U937 cells, but not in U937 cells stably expressing p21 antisense mRNA (Ref. 24; Fig. 7A). p21 antisense and control U937 cells were then treated with VPA for 7 days and evaluated for CD11b induction. CD11b was induced in a time- and dose-dependent manner in control cells, but not in cells lacking p21 (Fig. 7, *B* and *C*). These observations indicate that p21 is required for the response to VPA.

Differentiation of K562 Cells Induced by VPA and VPA Analogs. We have also analyzed the effects of VPA and analogs in K562 cells, a hematopoietic stem cell-like cell line that can be induced to differentiate toward the erythroid lineage by treatment with butyrate, hemin, or hydroxyurea and to megakaryocytic lineages by exposure to phorbol esters. Treatment with VPA for 3 days induced erythrocytic differentiation of K562 cells, as assessed by increased expression of fetal hemoglobin, glycophorin A, and the fraction of benzidine-positive cells (Fig. 8), but not the megakaryocytic marker CD41 (data not shown). 2EH and 4PA also induced glycophorin A and increased the fraction of benzidine-positive cells, whereas 2M2PP had a weak effect, and VPM and 2M2P had no effect (Fig. 8, *B* and *C*), again paralleling their potencies for *in vitro* inhibition of HDACs. These findings support the conclusion that HDAC is the target of VPA in the induction of differentiation in diverse transformed cell types.

Rapid Activation of MAPK in WRT Cells Is Pharmacologically Distinct from HDAC Inhibition. VPA has previously been found to activate the MAPK pathway, an effect that could be mediated through
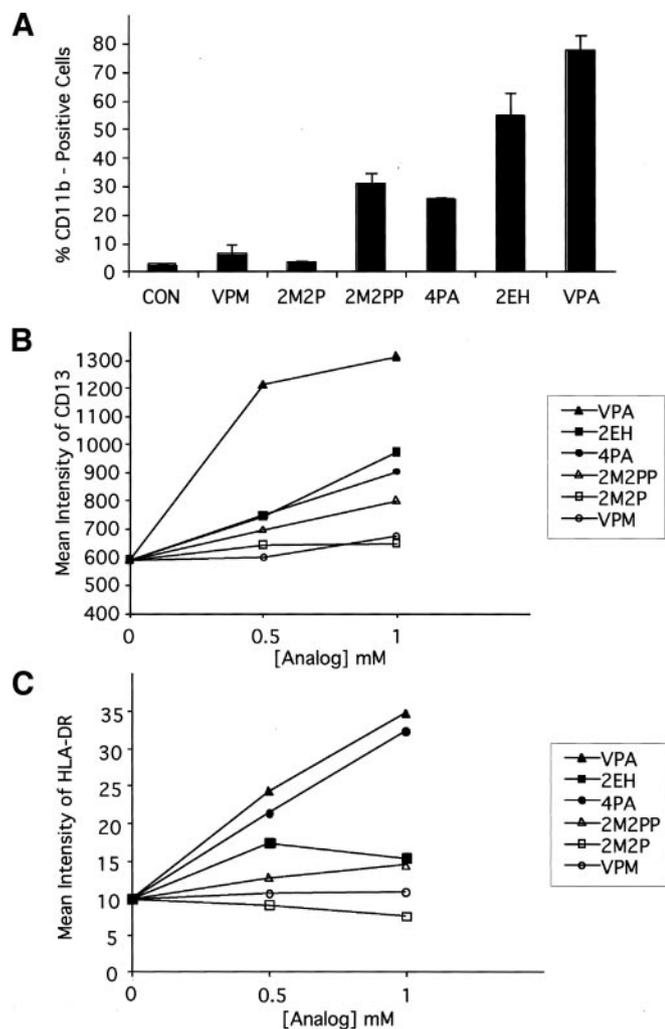
Fig. 6. Induction of differentiation in U937 cells by valproic acid (VPA) and VPA analogs. *A,* U937 cells were treated with 2 mM VPA or VPA analogs and analyzed for expression of CD11b by FCM. The percentage of CD11b-positive cells (as the mean of triplicate samples) ± SD was plotted. *B,* U937 cells were treated with VPA and analogs and evaluated for CD13 induction by FCM. Mean intensities were plotted for the indicated concentrations of VPA and analogs. *C,* U937 cells were treated with VPA and analogs and evaluated for HLA-DR expression by FCM. Mean intensities were plotted for the indicated concentrations of VPA and analogs.

on these observations, activation of MAPK by VPA in this setting likely occurs through a different mechanism. In addition, the data show that VPM and 2M2P, which were inactive in HDAC inhibition and cell differentiation assays, are nevertheless active in other cell-based assays. Thus, the lack of an effect on differentiation was not due to instability or inaccessibility of these compounds to the intracellular milieu.

DISCUSSION

Using a series of compounds with structural similarity to VPA, we have established a pharmacological profile for HDAC inhibition by VPA and its analogs. Applying this profile to the induction of differentiation in leukemia cell lines, we found that the relative potencies of VPA analogs to inhibit HDACs correlated with their potencies in inducing the differentiation of leukemia cell lines. Given this strong correlation and the similar effects of structurally unrelated HDAC inhibitors, we conclude that the effects of VPA on differentiation are most likely due to inhibition of HDACs. Similar to other HDAC inhibitors, VPA induced the cell cycle inhibitor p21, and, as observed previously for butyrate, the induction of differentiation in U937 cells was p21 dependent.
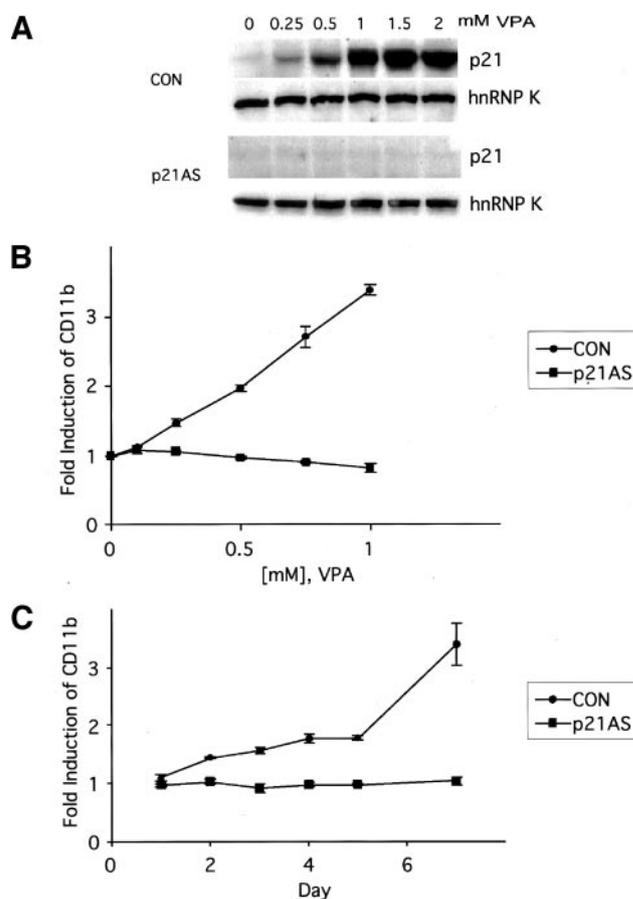

Fig. 7. p21 is required for the induction of differentiation by valproic acid (VPA) in U937 cells. *A,* stable U937 cell lines expressing either p21 antisense (*p21AS*) or empty vector control (*CON*; Ref. 24) were treated with 0.25–2 mM VPA for 24 h and immuno-blotted for p21 or hnRNP-K (loading control). A dose-dependent induction of p21 is evident in control cells but not in p21 antisense cells. *B,* control and p21 antisense cells were treated with 0.1–1 mM VPA for 6 days and analyzed for the expression of CD11b by FCM. CD11b was induced in control cells but not in p21 antisense cells. Fold induction of mean intensity of CD11b ± SD was plotted. The results are representative of three experiments. *C,* control and 0.5 mM VPA-treated U937 cells were analyzed for CD11b expression on days 1–5 and 7. CD11b expression increased in control but not p21 antisense cells treated with VPA. The data are represented as fold induction of mean intensity of CD11b after VPA treatment; each data point is the mean of triplicates ± SD.

HDAC inhibition, through other molecular targets of VPA, or both mechanisms. We examined activation of MAPK by VPA in Neuro2A and K562 cells and found apparent MAPK phosphorylation at approximately 1 h, but these studies were hampered by highly variable basal phosphorylation of MAPK in these cell types. We therefore focused on WRT cells, which displayed consistently low basal MAPK phosphorylation.

We find that VPA rapidly and robustly activates MAPK in WRT cells, as assessed by phosphorylation of MAPK (Fig. 9*A*). This VPA-induced phosphorylation is detectable within 2 min, maximal by 5 min, and returns to baseline within 60 min. To test whether this rapid response to VPA was pharmacologically similar to inhibition of HDACs, we examined the effect of VPA analogs on activation of MAPK in WRT cells. Butyrate did not activate MAPK at 2–60 min (Fig. 9*A*), suggesting that inhibition of HDACs does not activate MAPK under these conditions. Furthermore, the order of potency of other VPA analogs in the activation of MAPK was clearly distinct from the inhibition of HDACs. Thus, 2EH, 2M2P, 2M2PP, 4PA, and VPM activated MAPK more effectively than VPA, in sharp contrast to the profile for inhibition of HDACs shown above (Fig. 9*B*). Based

VPA has multiple effects in diverse systems. For example, in humans VPA is an anticonvulsant, a mood stabilizer, and a potent teratogen. In most cases, however, the targets responsible for these effects have not been defined (2). VPA can indirectly affect the function of a number of molecules, including PPARδ, β-catenin, activator protein 1, protein kinase C, and MAPK (12). VPA is also a direct inhibitor of several molecular targets, including HDACs, γ-amino butyric acid transaminase, and succinate semialdehyde dehydrogenase, as determined by *in vitro* assays (2). The pharmacological profile for HDAC inhibition by VPA analogs may therefore serve as a useful tool to investigate which effects of VPA arise through inhibition of HDACs. This pharmacological approach has been elegantly applied in rodents to distinguish the teratogenic activity of VPA from its anticonvulsant activity, strongly implying that different molecular targets mediate these two effects (19). A strong correlation was found between analogs that are teratogenic and those that can activate a PPARδ transcription reporter, whereas anticonvulsant activity did not correlate with teratogenicity (18). For example, VPM is an effective anticonvulsant in rodents, but it is not teratogenic (19). Furthermore, analogs previously shown to be teratogenic are effective HDAC inhibitors (3, 4). Based on these findings, the anticonvulsant activity of VPA is probably not a consequence of HDAC inhibition,
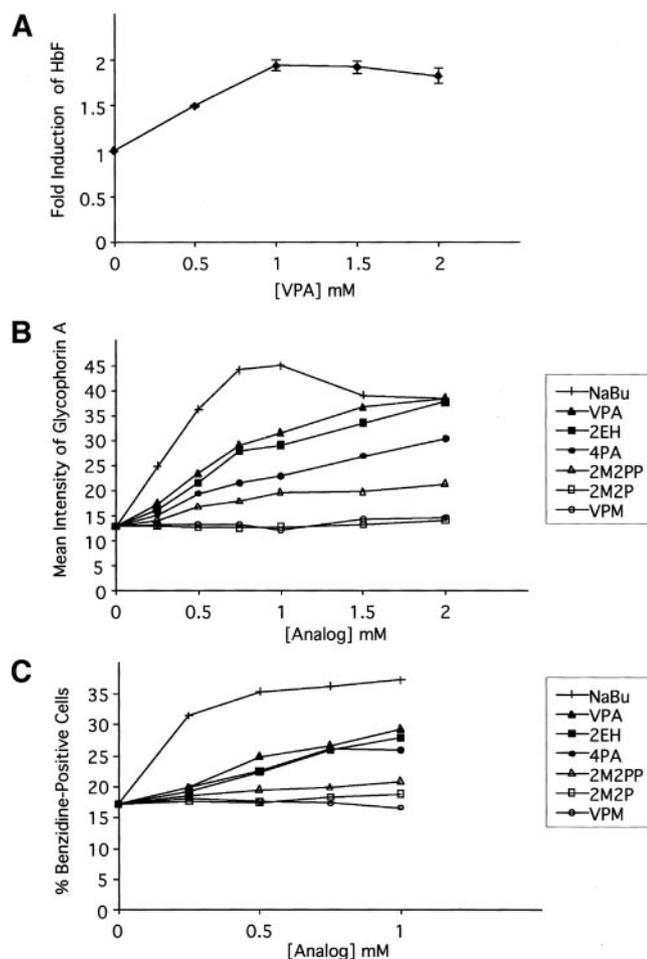

Fig. 9. Rapid activation of mitogen-activated protein kinase (MAPK) in Wistar rat thyroid (WRT) cells by valproic acid (VPA) analogs. *A,* WRT cells were treated with 2 mM VPA and sodium butyrate (*NaBu*), harvested at the indicated times, electrophoresed on 10% SDS-PAGE, and immunoblotted for phosphorylated MAPK (phospho-MAPK), which reflects activation of MAPK, as well as for actin (loading control). *B,* WRT cells were treated with 2 mM VPA analogs, harvested after 2 and 5 min, and immunoblotted for phospho-MAPK and actin (loading control).

but the teratogenic property has been proposed to be due to HDAC inhibition (3). This pharmacological approach has been extended here to test whether HDACs could be the direct targets of VPA-induced differentiation; we find a strong and consistent correlation between HDAC inhibition *in vitro*, endogenous histone acetylation *in vivo* (including local acetylation of p21 promoter-associated histones), activation of transcription, and induction of differentiation (see also Ref. 4), supporting the argument that HDACs are the relevant targets in this setting.

We also show that other VPA-mediated effects can be distinguished from HDAC inhibition. As others have described, we have observed activation of MAPKs after treatment with VPA and VPA analogs. Whereas VPA can activate MAPK, as determined by increased phosphorylation, in a variety of cell types, including WRT (Fig. 8), K562, Neuro2A, and 293T cells (data not shown), we chose the WRT cell line for further analysis because it showed reproducibly low basal activation/phosphorylation of MAPK. We observed a remarkably rapid phosphorylation of MAPK (within 2 min) in WRT cells, kinetics that are inconsistent with a process that would require new transcription or translation. Furthermore, the order of potency of VPA analogs in inducing this phosphorylation was clearly distinct from the profile for inhibition of HDACs, strongly suggesting that HDACs are not the target of VPA responsible for the robust activation of MAPKs in WRT cells. Rapid activation of MAPKs has also been described after treatment of K562 and neuroepithelioma CHP126 cells with butyrate (25–27); we did not observe MAPK activation with butyrate in WRT cells, and this my reflect cell type differences or differences in experimental conditions. In addition, VPA has been shown to activate MAPK in neuroblastoma SH-SY5Y cells after 24 h (28); whether this later activation of MAPK is due to HDAC inhibition remains to be examined. Thus, our observations do not rule out a role for HDAC inhibition in the activation of MAPKs in other cell types or after prolonged exposure, an intriguing possibility that will require further investigation. The important point here is that biochemical effects

Fig. 8. Induction of erythrocytic differentiation in K562 cells by valproic acid (VPA) and analogs. *A,* K562 cells were treated with the indicated concentrations of VPA and evaluated for expression of fetal hemoglobin (*HbF*) by FCM. Representative results from three independent experiments were plotted as fold induction of mean intensity of fetal hemoglobin ± SE. *B,* expression of glycophorin A in K562 cells treated with VPA or VPA analogs was evaluated by FCM and plotted as mean intensity. The result is representative of three independent experiments. *C,* percentage of benzidine-positive cells (of 300 cells counted) after treatment with VPA analogs at the indicated concentrations. The result shown is representative of three experiments.
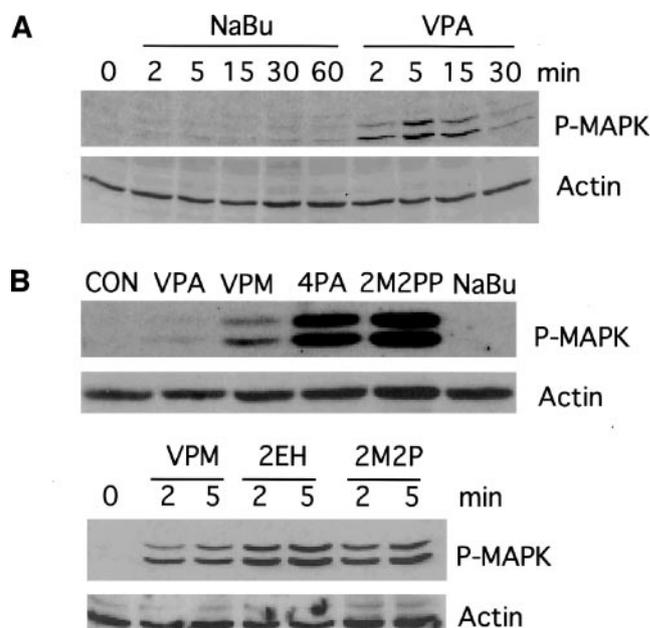
mediated by VPA can be distinguished using the analog profile described here and by others (as cited above).

In our assays, VPA does not inhibit HDAC6 or HDAC10 (HDACs from class II subclass II). These HDACs are structurally distinct from other class I and class II HDACs because they possess two domains similar to the catalytic domain of HDACs. HDAC6 possesses two active domains, whereas HDAC10 possesses one active and one inactive catalytic domain. Whereas the reason for the resistance of these HDACs to VPA is not clear, the presence of two domains could render the HDACs insensitive to inhibition by VPA. For example, HDACs 6 and 10 are also insensitive to butyrate, and when the inactive, COOH-terminal catalytic domain of HDAC10 was deleted, the truncated HDAC10 became sensitive to butyrate (16). Recently, HDAC6 was shown to associate with and regulate the acetylation of α-tubulin (29). Thus, VPA may be useful as a semiselective HDAC inhibitor that, similar to butyrate and distinct from other HDAC inhibitors such as TSA, does not interfere with the cytoplasmic function of HDAC6. Gottlicher *et al.* (4) have also reported that HDAC6 is less sensitive to VPA, although they did observe inhibition ($IC_{50} = 2.4$ mM), whereas the IC_{50} in our assays was >20 mM; the difference may reflect the different *in vitro* assays used or the source of HDAC6, and this issue remains under investigation.

HDAC inhibitors, including butyrate, TSA, suberoylanilide hydroxamic acid (SAHA), MS-27-275, and others, inhibit growth and induce differentiation in various cell culture models of cancer, including leukemia. Several HDAC inhibitors are currently in Phase I and Phase II clinical trials as cancer therapeutics (7, 8). However, the use of some of the established HDAC inhibitors is limited by their toxicity (30, 31). The recent finding that VPA is also a HDAC inhibitor suggests that it could serve as a valuable alternative differentiation agent because it is a clinically well-characterized and well-tolerated drug, and the IC_{50} for HDAC inhibition is well within its therapeutic range. Furthermore, VPA inhibits HDACs *in vivo* (32) and inhibits tumor growth and metastasis in rodents (4). Moreover, VPA is administered orally and has a half-life in humans of approximately 16 h [the half-life for the structurally related butyrate is approximately 5 min (33)]. In conclusion, we provide evidence that HDACs are the targets of VPA in the differentiation of hematopoietic cell lines; these findings suggest a role for VPA in the treatment of leukemias and other malignancies.

ACKNOWLEDGMENTS

REFERENCES

1. Johannessen, C. U. Mechanisms of action of valproate: a commentatory. Neurochem. Int., *37:* 103–110, 2000.
2. Gurvich, N., and Klein, P. S. Lithium and valproic acid: parallels and contrasts in diverse signaling contexts. Pharmacol. Ther., *96:* 45–66, 2002.
3. Phiel, C. J., Zhang, F., Huang, E. Y., Guenther, M. G., Lazar, M. A., and Klein, P. S. Histone deacetylase is a direct target of valproic acid, a potent anticonvulsant, mood stabilizer, and teratogen. J. Biol. Chem., *276:* 36734–36741, 2001.
4. Gottlicher, M., Minucci, S., Zhu, P., Kramer, O. H., Schimpf, A., Giavara, S., Sleeman, J. P., Lo Coco, F., Nervi, C., Pelicci, P. G., and Heinzel, T. Valproic acid defines a novel class of HDAC inhibitors inducing differentiation of transformed cells. EMBO J., *20:* 6969–6978, 2001.
5. Strahl, B. D., and Allis, C. D. The language of covalent histone modifications. Nature (Lond.), *403:* 41–45, 2000.
6. Grozinger, C. M., and Schreiber, S. L. Deacetylase enzymes: biological functions and the use of small-molecule inhibitors. Chem. Biol., *9:* 3–16, 2002.
7. Marks, P. A., Richon, V. M., Breslow, R., and Rifkind, R. A. Histone deacetylase inhibitors as new cancer drugs. Curr. Opin. Oncol., *13:* 477–483, 2001.
8. Kramer, O. H., Gottlicher, M., and Heinzel, T. Histone deacetylase as a therapeutic target. Trends Endocrinol. Metab., *12:* 294–300, 2001.
9. Gore, S. D., and Carducci, M. A. Modifying histones to tame cancer: clinical development of sodium phenylbutyrate and other histone deacetylase inhibitors. Expert Opin. Investig. Drugs, *9:* 2923–2934, 2000.
10. Cheson, B. D., Zwiebel, J. A., Dancey, J., and Murgo, A. Novel therapeutic agents for the treatment of myelodysplastic syndromes. Semin. Oncol., *27:* 560–577, 2000.
11. Cinatl, J., Jr., Cinatl, J., Scholz, M., Driever, P. H., Henrich, D., Kabickova, H., Vogel, J. U., Doerr, H. W., and Kornhuber, B. Antitumor activity of sodium valproate in cultures of human neuroblastoma cells. Anticancer Drugs, *7:* 766–773, 1996.
12. Blaheta, R. A., and Cinatl, J., Jr. Anti-tumor mechanisms of valproate: a novel role for an old drug. Med. Res. Rev., *22:* 492–511, 2002.
13. Kim, J. S., Lee, S., Lee, T., Lee, Y. W., and Trepel, J. B. Transcriptional activation of p21$^{WAF1/CIP1}$ by apicidin, a novel histone deacetylase inhibitor. Biochem. Biophys. Res. Commun., *281:* 866–871, 2001.
14. Richon, V. M., Sandhoff, T. W., Rifkind, R. A., and Marks, P. A. Histone deacetylase inhibitor selectively induces p21WAF1 expression and other gene-associated histone acetylation. Proc. Natl. Acad. Sci. USA, *97:* 10014–10019, 2000.
15. Hoffmann, K., Brosch, G., Loidl, P., and Jung, M. First non-radioactive assay for in vitro screening of histone deacetylase inhibitors. Pharmazie, *55:* 601–606, 2000.
16. Guardiola, A. R., and Yao, T. P. Molecular cloning and characterization of a novel histone deacetylase HDAC10. J. Biol. Chem., *277:* 3350–3356, 2002.
17. Barlow, A. L., van Drunen, C. M., Johnson, C. A., Tweedie, S., Bird, A., and Turner, B. M. dSIR2 and dHDAC6: two novel, inhibitor-resistant deacetylases in *Drosophila melanogaster.* Exp. Cell Res., *265:* 90–103, 2001.
18. Lampen, A., Siehler, S., Ellerbeck, U., Gottlicher, M., and Nau, H. New molecular bioassays for the estimation of the teratogenic potency of valproic acid derivatives in vitro: activation of the peroxisomal proliferator-activated receptor (PPARδ). Toxicol. Appl. Pharmacol., *160:* 238–249, 1999.
19. Nau, H., Hauck, R. S., and Ehlers, K. Valproic acid-induced neural tube defects in mouse and human: aspects of chirality, alternative drug development, pharmacokinetics and possible mechanisms. Pharmacol. Toxicol., *69:* 310–321, 1991.
20. Lin, R., Leone, J. W., Cook, R. G., and Allis, C. D. Antibodies specific to acetylated histones document the existence of deposition- and transcription-related histone acetylation in *Tetrahymena.* J. Cell Biol., *108:* 1577–1588, 1989.
21. Chen, W. Y., and Townes, T. M. Molecular mechanism for silencing virally transduced genes involves histone deacetylation and chromatin condensation. Proc. Natl. Acad. Sci. USA, *97:* 377–382, 2000.
22. Sambucetti, L. C., Fischer, D. D., Zabludoff, S., Kwon, P. O., Chamberlin, H., Trogani, N., Xu, H., and Cohen, D. Histone deacetylase inhibition selectively alters the activity and expression of cell cycle proteins leading to specific chromatin acetylation and antiproliferative effects. J. Biol. Chem., *274:* 34940–34947, 1999.
23. Archer, S. Y., Meng, S., Shei, A., and Hodin, R. A. p21^{WAF1} is required for butyrate-mediated growth inhibition of human colon cancer cells. Proc. Natl. Acad. Sci. USA, *95:* 6791–6796, 1998.
24. Rosato, R. R., Wang, Z., Gopalkrishnan, R. V., Fisher, P. B., and Grant, S. Evidence of a functional role for the cyclin-dependent kinase-inhibitor p21WAF1/CIP1/MDA6 in promoting differentiation and preventing mitochondrial dysfunction and apoptosis induced by sodium butyrate in human myelomonocytic leukemia cells (U937). Int. J. Oncol., *19:* 181–191, 2001.
25. Witt, O., Sand, K., and Pekrun, A. Butyrate-induced erythroid differentiation of human K562 leukemia cells involves inhibition of ERK and activation of p38 MAP kinase pathways. Blood, *95:* 2391–2396, 2000.
26. Yang, J., Kawai, Y., Hanson, R. W., and Arinze, I. J. Sodium butyrate induces transcription from the Gα_{i2} gene promoter through multiple Sp1 sites in the promoter and by activating the MEK-ERK signal transduction pathway. J. Biol. Chem., *276:* 25742–25752, 2001.
27. Espinos, E., and Weber, M. J. Activation of the MAP kinase cascade by histone deacetylase inhibitors is required for the stimulation of choline acetyltransferase gene promoter. Brain Res. Mol. Brain Res., *56:* 118–124, 1998.
28. Yuan, P. X., Huang, L. D., Jiang, Y. M., Gutkind, J. S., Manji, H. K., and Chen, G. The mood stabilizer valproic acid activates mitogen-activated protein kinases and promotes neurite growth. J. Biol. Chem., *276:* 31674–31683, 2001.
29. Hubbert, C., Guardiola, A., Shao, R., Kawaguchi, Y., Ito, A., Nixon, A., Yoshida, M., Wang, X. F., and Yao, T. P. HDAC6 is a microtubule-associated deacetylase. Nature (Lond.), *417:* 455–458, 2002.
30. Sandor, V., Bakke, S., Robey, R. W., Kang, M. H., Blagosklonny, M. V., Bender, J., Brooks, R., Piekarz, R. L., Tucker, E., Figg, W. D., Chan, K. K., Goldspiel, B., Fojo, A. T., Balcerzak, S. P., and Bates, S. E. Phase I trial of the histone deacetylase inhibitor, depsipeptide (FR901228, NSC 630176), in patients with refractory neoplasms. Clin. Cancer Res., *8:* 718–728, 2002.
31. Marks, P., Rifkind, R. A., Richon, V. M., Breslow, R., Miller, T., and Kelly, W. K. Histone deacetylases and cancer: causes and therapies. Nat. Rev. Cancer, *1:* 194–202, 2001.
32. Tremolizzo, L., Carboni, G., Ruzicka, W. B., Mitchell, C. P., Sugaya, I., Tueting, P., Sharma, R., Grayson, D. R., Costa, E., and Guidotti, A. An epigenetic mouse model for molecular and behavioral neuropathologies related to schizophrenia vulnerability. Proc. Natl. Acad. Sci. USA, *99:* 17095–17100, 2002.
33. Blaheta, R. A., Nau, H., Michaelis, M., and Cinatl, J., Jr. Valproate and valproate-analogues: potent tools to fight against cancer. Curr. Med. Chem., *9:* 1417–1433, 2002.